

Historic, Archive Document

Do not assume content reflects current
scientific knowledge, policies, or practices.

Journal
A99.9
F76324

CORE LIST

USDA Forest Service
Research Paper RM-152
Rocky Mountain Forest and
Range Experiment Station
Forest Service
U.S. Department of Agriculture
Fort Collins, Colorado 80521

September 1975

Heat and Water Vapor Flux in Conifer Forest Litter and Duff: A Theoretical Model

Michael A. Fosberg

U.S. DEPT. OF AGRICULTURE
NATIONAL FOREST SERVICE
FBI 28 75
GENERAL RECORDS

Abstract

Fosberg, Michael A.

1975. Heat and water vapor flux in conifer forest litter and duff: a theoretical model. USDA For. Serv. Res. Pap. RM-152, 23p. Fort Collins, Colo. 80521.

The model was developed from numerical and analytical solutions of the diffusion forms of the mass continuity equation and the first law of thermodynamics. Analytical solutions provided a functional framework to evaluate nonlinear interactions obtained in the numerical solutions. Dimensional analysis was used to define the relationships between the soil properties used in the model.

Keywords: Soil physics, forest fires, forest fuels.

669038

USDA Forest Service
Research Paper RM-152

September 1975

U. S. DEPT. OF AGRICULTURE
NATIONAL AGRICULTURAL LIBRARY

FEB 26 1976

CATALOGING • PREP.

2007
Heat and Water Vapor Flux in Conifer Forest Litter and Duff:

A Theoretical Model¹ C.D.

Michael A. Fosberg, Principal Meteorologist
Rocky Mountain Forest and Range Experiment Station²

¹From a thesis submitted to the Graduate Faculty of Colorado State University in partial fulfillment of the requirements for the degree of Doctor of Philosophy.

²Central headquarters is maintained at Fort Collins, in cooperation with Colorado State University.

Contents

	Page
Introduction	1
Analysis of Previous Work	1
Structure of the Model	2
The Mathematical Model	3
Idealized Analytical Solutions	6
Relation of Timelag to Physical Properties	8
Numerical Solution Methods	9
Results of the Computations	10
Constant Boundary Conditions	11
Time-Dependent Boundary Conditions	16
Comparison of Generalized Solutions with Fickian Solutions	16
Conclusions	18
Literature Cited	19
Appendix	21

Heat and Water Vapor Flux in Conifer Forest Litter and Duff: A Theoretical Model

Michael A. Fosberg

Introduction

The uppermost layers of the forest floor are a complex interactive component of the natural water balance. The organic particles found in these layers have water sorption properties that depend on their previous state and on the chemistry and cellular structure of the parent organic material. The physical structure of the layers depends also on the microclimate of the forest stands, as well as the physiology-dependent organic decay rates of the particles.

These particles are rarely in equilibrium with the microenvironment of the soil voids, and almost never in equilibrium with the external environmental stresses imposed by the atmosphere. Organic soil particles respond to the soil void microenvironment more slowly than changes in that void environment. An individual organic soil particle is both a source and sink for water and energy in a complex, dynamic system. Latent and sensible heat exchange and mass conservation of water take place simultaneously and interact between the particles, soil voids, and the external environment. These processes must be accounted for through an interactive model to physically depict the processes in accurate detail.

Wildfire behavior and damage are strongly influenced by the moisture content of the organic forest soils. Prescribed fire for removal of the litter and duff for seedbed preparation, and for hazard reduction through removal of the understory also depends on the litter and duff moisture content. Reliable means of predicting the moisture contents of litter and duff are required for predicting effort required in wildfire control and for safe, beneficial use of prescribed fire.

In this Paper, a theoretical model based on conservation of energy and mass was developed for predicting the moisture content of litter and duff under high moisture stress. The prediction model was obtained by first considering restrictive analytical solutions of simple functions for diffusion of single layers of porous media. These simple solutions for fixed boundary conditions defined a general equation to evaluate timelags from numerical solutions of nonlinear differential equations. The boundary conditions were then relaxed and allowed to vary as small time-dependent step functions in a second analytical solution. This solution defined a more general case, and provided the bases for

numerical experiments with the nonlinear equations with variable boundary conditions to evaluate and calibrate the coefficients of the solution. This general solution represented the response of the litter and duff to natural environmental stresses, and provided the functional framework for predicting the moisture and temperature profiles.

Analysis of Previous Work

Soil moisture and heat transfer analysis has traditionally been applied to saturated or partially saturated soils. This emphasis on the presence of liquid-water transfer stems from agricultural needs for moisture in the root zone, and for conservation of impounded water. While the complete processes of heat and mass transfer between soil particles and soil voids and between adjacent voids are qualitatively known, most previous quantitative work has concentrated on the processes associated with liquid water (Chudnovskii 1962, Childs 1969). Under these conditions, the largest mass of soil water is in the soil voids, and the moisture bound within and on the soil particles contributes little to the water balance as sources or sinks of moisture. Because of this emphasis on liquid water, most analytical and theoretical work has been based on a simple Darcy type of flow where the soil structure can be accounted for by simple diffusivity or hydraulic conductivity. The assumption that the particles do not contribute materially to the water and energy budgets breaks down if no liquid water is present, because the total heat content and moisture in the voids is small compared to those in the particles (USDA-FPL 1974, Jackson 1964c).

Studies of soil aeration with nonsorbing porous media demonstrated that the diffusion rates of gases and vapors are a substantial fraction of the molecular diffusion rates in free air. The diffusion of gases in porous media may be as high as 10 percent of that in free air, even with porosities as low as 15 percent (Penman 1940; Taylor 1949; Millington 1959; Currie 1960a, 1960b, 1961; Millington and Scheerer 1971; Ayres *et al.* 1972). For porosities of 70 to 90 percent, the range common to duff and litter, the diffusion rate is 60 to 80 percent of that in the free air. Thus, soils in general and litter and duff horizons in particular do not markedly reduce the gas exchange by their structure.

Experimental determinations of soil-void vapor diffusivities with sorbing materials have produced mixed results; studies by de Jong and Schappert (1972) and Hanks (1958) show agreement with the nonsorbing materials. Jackson (1964a, 1964b) calculated diffusivities two to three orders of magnitude lower than those found in nonsorbing experiments. Jackson's (1964c) steady state experiments provide a clue on how to reconcile this discrepancy. The sorption isotherms indicate that the soil particles contain substantial amounts of water in comparison with that contained in the voids at equilibrium. Jackson assumed that the particles are always in equilibrium with the voids. If the exchange of moisture between the voids and particles is time dependent (lags behind), then use of the equilibrium isotherms to evaluate the diffusivity will underestimate the diffusivity in the voids. If the particles respond very slowly to stress, then the estimate of diffusivity will be very low. Only as their response rate approaches the instantaneous will the equilibrium isotherm technique be valid. Therefore, one must know the response rates of individual particles as well as the bulk diffusivities of the soil matrix to calculate the heat and mass exchange.

Two sets of characteristics of particle behavior need to be defined to properly account for heat and mass transfer between the particles and voids: timelags and equilibrium isotherms. The timelag is defined through the time interval during which a particle will gain or lose heat or moisture from a homogeneous state after a specific change in the environment. The change takes place as an exponential decay to the new equilibrium condition. The timelag is then defined as the time interval required to achieve $1-1/e$ (approximately 62 percent) of the potential change. Theoretical analysis under laboratory conditions has defined the timelag in terms of particle properties (Byram,³ Fosberg 1970). This theoretical work was extended to field situations by generalizing the boundary conditions in the solutions (Fosberg 1972, 1973). The equations in Fosberg (1972) provide the basis for moisture exchange in the soil particles, and the equations in Fosberg (1973) do the same for heat exchange. Moisture timelags for many of the litter and duff particles have been analyzed by Nelson (1969), Van Wagner (1969), Fosberg (1970), and Mutch and Gastineau (1970). Data on thermal timelags are far less available. The only compilation for organic materials is in Fosberg (1973). Unfortunately, no data exist for either moisture or thermal timelags of soil particles.

The second set of characteristics that must be known are the equilibrium isotherms for moisture and specific heat of the soil, litter, and duff particles. These isotherms define the boundary conditions required for heat and water exchange. The equilibrium moisture iso-

therms for soil particles have been compiled by Baver (1956), Jackson (1964c), and Miyamoto *et al.* (1972). As with the timelags, there are numerous sources of equilibrium isotherm data for woody materials. The USDA Forest Products Laboratory (1974) has compiled a comprehensive set of tables for commercial woods. Data for fine particles found in litter and duff are presented in Mutch and Gastineau (1970) and Blackmarr (1971). The thermal properties of soil particles are well documented in soil texts (Baver 1956, Chudnovaskii 1962) and those of woody materials in Siau (1971).

Analysis of the soil physics and fuel moisture literature lead directly to a conceptual model of energy and vapor flow in forest litter and duff. The particles respond slowly to changes in the void microenvironment, while the environment of the voids can change rapidly. This process was recognized near the beginning of fuel moisture research. Early papers clearly defined the litter and duff as well aerated (Gast and Stickel 1929) and stated that the particle response lagged behind changes in humidity (Harkness 1939). This slow response of litter and duff particles to liquid water was observed more recently by Clary and Ffolliott (1969). Most of the recent work on duff and litter moisture, particularly that intended for predictive methods, has departed from relations depicting the physical processes, and have concentrated on developing a drought index or build-up index. The approach with the synthetic indices required regression equations to relate the indices to duff and litter (Jarvis and Tucker 1968, Johnson 1968, Muraro and Lawson 1970). While this approach provides easily used tools, the indices are not directly related to duff and litter moisture, and a new set of regressions must be obtained for each site. Van Wagner (1970) approached the prediction problem by a method more closely related to the physical processes. Because he used a mathematical model developed for fixed boundary conditions, his model does not fully depict the physical processes. Van Wagner transformed the model from a constant environment solution to a field solution through a variable timelag. This variable timelag combined both the lag produced by the physical structure and the variations in moisture change produced by a varying environment.

Structure of the Model

Four distinct processes take place simultaneously in the litter and duff system. The organic particles exchange heat and water vapor with the surrounding voids. The exchange rates are determined by (a) the boundary conditions imposed by the temperature and relative humidity in the voids, (b) the excess or deficit of heat and moisture in the particles in comparison to the boundary condition imposed by the void atmosphere, and (c) the rate at which the particles can take up or give off heat and water vapor. The last two pro-

³Byram, George M. 1963. *An analysis of the drying process in forest fuel materials. Paper presented at the 1963 International Symposium on humidity and moisture. Wash. D.C. May 20-23, 1963. 38 p.*

cesses involve exchange of heat and water vapor between adjacent voids in response to the concentration gradients.

The processes at a given level in the system are illustrated schematically in figure 1. The four corners represent the state variables of heat and vapor in the particles and in the voids. The bold, horizontal double-headed arrows define the dynamic processes of exchange between the particles and the voids. The bold vertical arrows indicate the exchange between adjacent voids. The light arrows and interior cells define the flow of energy and vapor and the interactive process of exchange between the particles and voids. The absolute moisture content and temperature of the voids specify the relative humidity of the voids. The void relative humidity in turn specifies the equilibrium moisture content that the particles would eventually achieve. This equilibrium moisture content represents, then, the environment to which the particles must respond, and is expressed as the boundary condition from the vapor transfer in to or out of the particles.

The transfer of vapor in to or out of a particle depends on the magnitude and direction of the difference between the actual particle moisture content and its equilibrium moisture content. The particles do not respond instantaneously to changes in the environment. The rate of response is expressed through the timelag in a quasi-exponential approach to the equilibrium.

librium. The particle timelag contains the information of size, internal moisture diffusivity, and shape of the particle. Heat transfer proceeds in a similar manner.

The temperature and heat content of the voids define the boundary condition imposed on the particles. Like the moisture exchange between the particles and voids, heat transfer depends on the temperature gradient and on the physical characteristics of size, shape, and specific heat. In addition, constraints are imposed by the influence of moisture on the thermal properties and by the second law of thermodynamics because of the large difference in specific heats. The particle moisture content influences the heat exchange through effects on the specific heat and through volumetric changes of the particles. Also, because of the large differences in specific heats and because heat cannot be moved against a temperature gradient, the laws of conservation of heat and mass governing the processes must be supplemented with the second law of thermodynamics.

The Mathematical Model

This descriptive model of heat and vapor transfer in duff and litter is based on two underlying concepts: (1) diffusive exchange between voids is rapid, and (2) exchange between voids and particles is slow, and is the

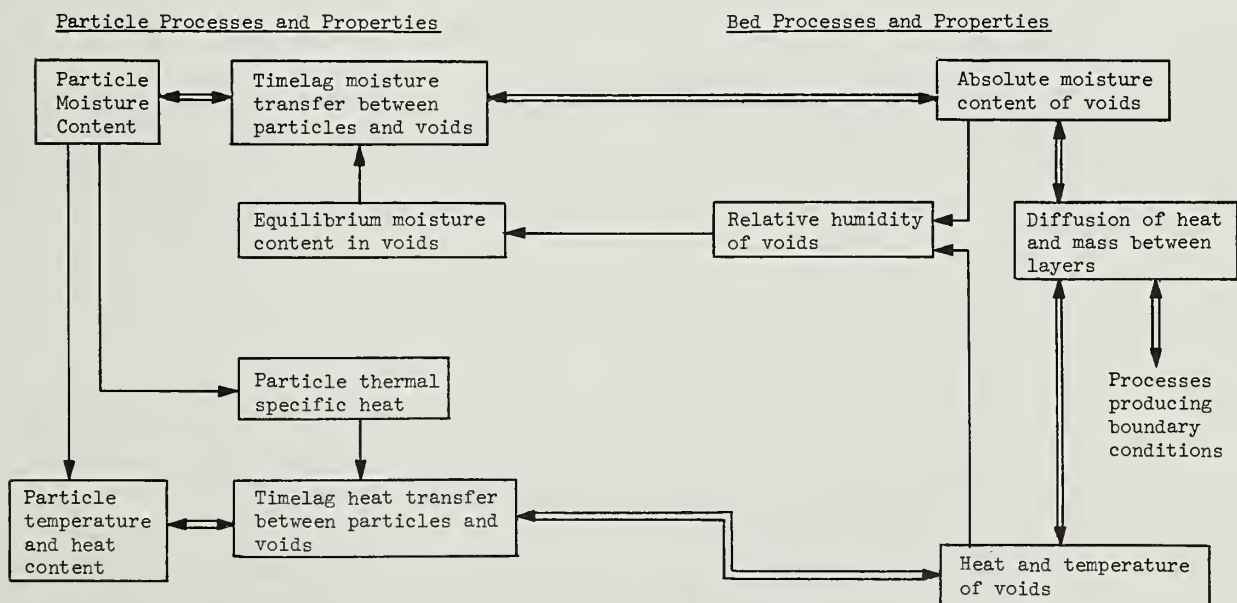


Figure 1.—Schematic diagram of heat and mass transfer processes in the internal layers of conifer forest litter and duff.

limiting factor in heat and vapor exchange. A theoretically derived model can now be constructed from these descriptive concepts.

The transport of water vapor through the voids is governed by the conservation of mass equations, where changes in density depend on diffusion of mass and on the vapor taken up or given off by the individual particles. The continuity equation for vertical transport in a horizontally homogeneous layer is:

$$\frac{\partial \rho_v}{\partial t} = \nu \frac{\partial^2 \rho_v}{\partial z^2} + \frac{\partial \nu}{\partial z} \frac{\partial \rho_v}{\partial z} \pm \chi$$

where ρ_v is the density of water vapor in the voids, ν is the molecular diffusivity governing the transport between voids, and χ is the rate of exchange of water vapor between the particles and the voids. The moisture content of the litter and duff particles is expressed on an oven-dry gravimetric base. Gain or loss of moisture content by the particles must be transformed to units consistent with those of the continuity equation. The moisture content of the particle is expressed as the mass of water divided by the oven-dry mass of the particle, and the vapor density is expressed as the mass of water vapor in the void volume. The particle moisture content is transformed to equivalent vapor density through multiplication by the bulk density of the layer and division by the porosity:

$$m \frac{\rho_B}{\phi} = \rho'_v$$

where m is the particle gravimetric content, ρ_B is the layer bulk density, and ϕ is the porosity. The relationship between particle changes in moisture and the corresponding moisture taken up or given off to the voids is now obtained by differentiation and thus defines the source or sink term χ .

$$\left[\frac{\rho_B}{\phi} \right] \frac{dm}{dt} = \frac{d\rho'_v}{dt} = \chi$$

The changes in particle moisture content produced by environmental stress derived by Fosberg (1972) are:

$$\frac{\Delta m}{\Delta t} = 1 - \zeta_m \exp \left[- \frac{t}{\tau_m} \right]$$

where δm is the actual moisture exchange, Δm is the potential exchange if the particle responded instantaneously, ζ is a coefficient reflecting the internal distribution of moisture, τ_m is the particle timelag, and t is the time over which the environmental stress acts. The particle moisture exchange may be differentiated and substituted directly into the continuity equation. Since the continuity equation is nonlinear, it will be solved by finite difference methods; this form of the equation is

appropriate provided t is replaced by δt , the finite time step. The continuity equation for water vapor is, therefore:

$$\frac{\partial \rho_v}{\partial t} = \nu \frac{\partial^2 \rho_v}{\partial z^2} + \frac{\partial \nu}{\partial z} \frac{\partial \rho_v}{\partial z} - \chi \quad [1]$$

where χ is approximated over a small finite interval by

$$\chi = \frac{\delta m \rho_B}{\phi} \quad [2]$$

and

$$\delta m = m - m_1 = \left(m e^{-m_1} \right) \left(1 - \zeta_m \exp \left(- \frac{\delta t}{\tau_m} \right) \right) \quad [3]$$

The transfer of heat through the voids is governed by the first law of thermodynamics. Since the particular problem is concerned with a shallow system vertically, the first law may be approximated as

$$c_p \frac{dT}{dt} - \frac{1}{\rho_a} \frac{dp}{dt} \approx c_p \frac{dT}{dt} = s$$

where c_p is the specific heat at constant pressure, T is the temperature, and s is the source or sink of heat provided by the particles. As with the water vapor, the heat is exchanged between voids by diffusion. The first law of thermodynamics is:

$$c_p \frac{\partial T}{\partial t} = c_p k \frac{\partial^2 T}{\partial z^2} + c_p \frac{\partial k}{\partial z} \frac{\partial T}{\partial z} \pm s$$

where k is the molecular diffusivity in the voids.

The thermal source or sink of heat provided by the litter and duff particles is also obtained from the first law of thermodynamics. Since energy must be conserved, any exchange of heat must be equal.

$$\delta H_F = \delta H_a$$

The total heat of the air is:

$$\delta H_a = M_a c_p \delta T_a$$

where H_a is the heat content of the voids, M_a is the mass of air in the voids, and T_a is the void air temperature. Similarly, for the particles:

$$\delta H_F = M_F c_F \delta T_F$$

and the void heat change is:

$$c_p \delta T_a = \frac{M_F c_F \delta T_F}{M_a}$$

Now, by multiplying this expression by a sequence of unity ratios:

$$c_p \delta T_a = \frac{M_F c_F \delta T_F}{M_a} \left(\frac{V_F}{V_F} \right) \left(\frac{V_v}{V_v} \right) \left(\frac{V_B}{V_B} \right) = \frac{\rho_F}{\rho_a} \frac{(1 - \phi)}{\phi} c_F \delta T_F$$

The heat exchange is expressed in terms of readily available properties. The V 's refer to volume and the subscripts F, V, and B represent particle, void, and total bed, respectively.

The dynamic response of temperature changes in the particles is given in Fosberg (1973) and is:

$$\frac{\delta T}{\Delta T} = 1 - \zeta_T \exp \frac{-t}{\tau_T}$$

where δT is the actual temperature change, and ΔT is the potential change for an instantaneous response, ζ_T is the internal distribution coefficient, and τ_T is the thermal response time or timelag.

Because $\rho_F c_F$ is much greater than $\rho_a c_p$, the second law of thermodynamics must also be considered. It is not necessary to quantitatively consider the second law in the numerical solutions, however. If the time step is selected sufficiently small, so that the heat flow from the high temperature to the lower temperature is maintained in the finite difference calculation, it is sufficient to calculate the heat exchange based only on the first law. The equation for temperature change in the voids is:

$$-\frac{\partial T}{\partial t} = k \frac{\partial^2 T}{\partial z^2} + \frac{\partial k}{\partial z} \frac{\partial T}{\partial z} - \frac{s}{c_p} \quad [4]$$

The temperature change in the voids by exchange with the particles is then

$$s = \delta T_F \frac{\rho_F (1 - \phi) c_F}{\rho_a \phi} \quad [5]$$

and the temperature change in the particles is

$$\delta T_F = T_F - T_{F1} = \left(T - T_{F1} \right) \left(1 - \zeta_T \exp \left(\frac{-\delta t}{\tau_T} \right) \right) \quad [6]$$

Equations [1] through [6] define the four dynamic processes of heat and vapor change and the two sets of relations between void and particle exchange. The equation of continuity [equation 1] and the first law of thermodynamics [equation 4] define the void-to-void exchange in terms of void properties and gains from or losses to the individual particles. The gain or loss of water vapor by the particles is given by equation

[3] and the gain or loss of temperature is given by equation [5]. The interface of mass exchange between equation [1] and equation [3] is given by equation [2]. The conservation of heat exchange with the restriction of preserving the second law of thermodynamics is given in equation [5]. With these six equations, the moisture and temperature profile dynamics are fully defined.

These equations must be supplemented by a set of diagnostic state equations to fully close the system. These diagnostic equations relate the void air thermodynamics properties to the void stresses imposed by relative humidity on the moisture and the heat content of the particles. The boundary condition of moisture transfer is defined as the equilibrium moisture content. This equilibrium moisture content is strongly dependent on relative humidity. Since the temperature and vapor density are known at any given time and point, the equations of state

$$e = \rho_v R_v T \quad [7]$$

can be used to calculate the vapor pressure in the voids. At constant pressure, the saturation vapor pressure is a function of temperature only. The saturation vapor pressure is calculated from the Goff-Gratch formulation presented in the Smithsonian meteorological tables (List 1966) and is reproduced here for completeness. The saturation vapor pressure is

$$\begin{aligned} \log_{10} e_s = & 1.790298 \left(\frac{T_s}{T} - 1 \right) \\ & + 5.02808 \log_{10} \left(\frac{T_s}{T} \right) \\ & - 1.3816 \times 10^{-7} \left(10^{11.344} \left(1 - \frac{T}{T_s} \right) - 1 \right) \\ & + 8.1328 \times 10^{-3} \left(10^{-3.4919} \left(1 - \frac{T}{T_s} \right) - 1 \right) \\ & + \log_{10} e_{ws} \end{aligned} \quad [8]$$

where T_s is the boiling point temperature (373.16°K) and e_{ws} is the saturation pressure of ordinary water at the boiling point temperature (1.013246×10^3 dynes cm^{-2}). The relative humidity (h) is then specified by:

$$h = \frac{100e}{e_s} \quad [9]$$

The boundary condition required for vapor flux to and from the particles is expressed by the equilibrium moisture content. Values of the equilibrium moisture content of softwoods as a function of temperature and relative humidity are given in the *Wood*

Handbook (USDA-FPL 1974). Equilibrium isotherms for pine needles were obtained from unpublished results of Blackmarr.⁴

The only other function needed to close the set of equations is the relation for specific heat of the particles. The specific heat according to Siau (1971) is:

$$c_F = \frac{m + 0.324}{1 + m} \text{ cal gm}^{-1} \text{ }^{\circ}\text{C}^{-1} \quad [10]$$

The diffusion of water vapor or heat through the voids is predicted from Millington and Scheerer's (1971) tortuosity factor. They determined that the vapor and thermal diffusivities would be reduced from the free air values by the ratios:

$$\frac{\nu}{\nu_o} = \phi^{2x} \quad [11a]$$

and

$$\frac{k}{k_o} = \phi^{2x} \quad [11b]$$

where the exponent x is defined by the implicit relation

$$\phi^{2x} = 1 - (1 - \phi)^x \quad [12]$$

If equation [12] is solved for x by relaxation, then the vapor diffusivity ν and thermal diffusivity k in the voids are defined by the values they would have in the free air. These free air values are indicated by the subscript o .

These predictive and diagnostic equations are highly interdependent and must be solved simultaneously. Because of the nonlinear character of the basic void diffusion equations, they must be solved numerically in order to obtain valid prediction of duff and litter moisture.

The procedures required to produce meaningful solutions from these equations require a number of separate solutions which are combined at various stages to provide the general models and the associated coefficients. Two distinct models were developed. The first was for heat and vapor flux under constant boundary conditions as might be carried out in a laboratory. This model was obtained first by developing simple analytical solution. This analytical solution was then refined by a series of numerical solutions to refine the analytical coefficients. Similarity solutions were then developed which predicted the laboratory timelags from the physical properties. The numerical values used to

develop the similarity relationship came from computer simulations. This model provided four equations. The first two predicted the time-dependent behavior of heat and vapor change in the porous bed, and the second two provided the heat and mass timelags from physical structure.

The second model was developed to transform the laboratory-type solution to field situations where the boundary conditions are continually changing. As in the laboratory model, this model was developed from analytical and numerical solutions. The analytical solution was obtained through the philosophy previously presented in Fosberg (1972) where the structural and environmental influences were separated. Timelags obtained in the first model were then used as a basis for evaluating environmental changes through numerical solutions. This model provided two time-dependent equations to be used with the similarity solution of the first model. Two coefficients of environmental influence were also defined covering heat and vapor flux.

Idealized Analytical Solutions

First, a simplified set of equations was solved analytically. These analytical solutions are gross simplifications of the real world situation. They are useful in that they provide a framework in which to evaluate the numerical solutions, and they define the types of numerical simulations that are required to obtain a prediction system of equations.

The analytical solutions were derived from simplified forms of equations [1] and [4]. In addition, the source and sink of energy or mass were neglected. Thus the analytical solutions represent Fickian diffusion through an inert porous media—one in which the particles respond instantaneously to pore micro-environmental changes. With these initial assumptions, the general form of equations [1] and [4] reduced to

$$\frac{\partial q}{\partial t} = D \frac{\partial^2 q}{\partial z^2} \quad [13]$$

Here, q represents either the vapor density of equation [1] or the temperature of equation [4], and D is either the vapor or thermal diffusivity. If a non-dimensional variable R is defined as

$$R(t, z) = \left(\frac{q(t, z) - q_e(z)}{q_o - q_e(z)} \right)$$

then R lies between 0 and 1. The variable $q_e(z)$ represents the final equilibrium state and q_o is the initial homogeneous value of q at time 0.

⁴Blackmarr, W. H. November 27, 1972, personal correspondence.

The diffusion equation [13] becomes:

$$\frac{\partial R}{\partial t} = D \left[\frac{\partial^2 R}{\partial z^2} - \frac{\partial R}{\partial z} \left(\frac{2 \frac{\partial q_e}{\partial z}}{(q_o - q_e)} \right) - \frac{\partial^2 q_e}{\partial z^2} \frac{(R-1)}{(q_o - q_e)} \right] \quad [14]$$

when expressed in nondimensional forms of q . The first derivative of R with respect to z may be eliminated by letting

$$R = Q \exp \left(\frac{1}{2} \int^2 \frac{\frac{\partial q_e}{\partial z}}{(q_o - q_e)} dz \right)$$

With this substitution, equation [14] becomes

$$\frac{\partial R}{\partial t} = D \left[\frac{\partial^2 R}{\partial z^2} + R \left(\frac{\partial^2 q_e}{\partial z^2} [1 - a] + \left(\frac{\frac{\partial q_e}{\partial z}}{(q_o - q_e)} \right)^2 + \frac{\frac{\partial^2 q_e}{\partial z^2}}{(q_o - q_e)} \right) \right] \quad [15]$$

when a is defined as

$$a = (q_o - q_e) \exp \left(\frac{1}{2} \int^2 \frac{\frac{\partial q_e}{\partial z}}{(q_o - q_e)} dz \right)$$

If this idealized solution is assumed to have fixed boundary conditions for q at the top and bottom, then the q_e profile is linear and the second derivatives of q_e vanish.

This assumption then allows equation [15] to be reduced further to

$$\frac{\partial R}{\partial t} = D \left[\frac{\partial^2 R}{\partial z^2} + R \left(\frac{\left(\frac{\partial q_e}{\partial z} \right)^2}{(q_o - q_e)} \right) \right] \quad [16]$$

Equation [16] may now be solved by separation of variables. We let R equal the product of two functions, one dependent only on time and one only on depth,

$$R = T(t) Z(z)$$

so that equation [16] is

$$\frac{Z}{D} \frac{\partial T}{\partial t} = T \frac{\partial^2 Z}{\partial z^2} + b^2 TZ \quad [17]$$

where

$$b^2 = \frac{\left(\frac{\partial q_e}{\partial z} \right)^2}{(q_o - q_e)}$$

Equation [17] then becomes

$$\frac{1}{TD} \frac{\partial T}{\partial t} = \frac{1}{Z} \frac{\partial^2 Z}{\partial z^2} + b^2 = -\alpha^2$$

or

$$\frac{1}{T} \frac{\partial T}{\partial t} = -\alpha^2 D \quad [18]$$

and

$$\frac{\partial^2 Z}{\partial z^2} + (b^2 + \alpha^2) Z = 0 \quad [19]$$

The solutions of equations [18] and [19] are

$$T = \exp(-\alpha^2 D t)$$

and

$$Z = A \exp((b+i\alpha)z) + B \exp((b-i\alpha)z)$$

so that

$$R = TZ = \exp(-\alpha^2 D t) [A \exp((b+i\alpha)z) + B \exp((b-i\alpha)z)]$$

The real part of this solution is

$$R = \exp(-\alpha^2 D t) \exp(bz) [C_1 \cos \alpha z + C_2 \sin \alpha z] \quad [20]$$

The boundary and initial conditions imposed on equations [20] are

$$R(0, z) = 1$$

$$R(t, 0) = 0$$

$$R(t, H) = 0$$

First applying the boundary condition at $z = 0$

$$0 = \exp(-\alpha^2 D t) C_2$$

and at

$$z = H$$

$$0 = \exp(-\alpha^2 D t) \exp(bH) \sin \alpha H$$

thus

$$\alpha = \frac{n\pi}{H}$$

and

$$R = \sum_{n=1}^{\infty} C_n \exp\left(-\frac{n^2\pi^2}{H^2} Dt\right) \exp(bz) \sin \frac{n\pi}{H} z \quad [21]$$

The general form of the diffusion processes is obtained by integrating R over the depth of the layer to obtain the integral mean value

$$\begin{aligned} \hat{R} &= \frac{1}{H} \int_0^H R dz \\ &= \frac{\sum_{n=1}^{\infty} C_n \exp\left(-\frac{n^2\pi^2}{H^2} Dt\right) \frac{n\pi}{H^2} (1-e^{-bH})}{\left(b^2 + \frac{n^2\pi^2}{H^2}\right)} \end{aligned} \quad [22]$$

This integration shows that an exponential approach to equilibrium should be expected. Thus a simplified form of equation [22] is

$$\hat{R} = \zeta \exp\left(-\frac{t}{\tau_B}\right) \quad [23]$$

where τ_B is timelag of the diffusion process. The constant ζ equals 1 since at time zero \hat{R} equals 1. This analytical solution applies only to conditions in which the external environment is held constant and the internal dynamic properties are initially uniform. This solution provides the basis for evaluation of the system dynamics as they would be investigated in the laboratory.

The laboratory type solution is difficult to apply to the field situation since it requires constant boundary conditions. Therefore a second analytical solution is derived which defines the functional form of the dynamics with nonstationary boundary conditions and a nonuniform initial condition. This solution is obtained by allowing the initial quantity to be a function of z . The boundary conditions are held constant over some small arbitrary interval of time. The value of q from the previous solution then becomes the q_0 for the new solution, and a new set of boundary conditions is applied.

The solution for this situation proceeds along the same lines as that for the homogeneous case. The non-dimensional variable R is now defined as:

$$R(t, z) = \frac{(q(t, z) - q_e(z))}{(q_0(z) - q_e(z))}$$

and is substituted into equation [13]. As in the previous solution, R is redefined as

$$R = Q \exp\left(-\frac{1}{2} \int_0^z \frac{\left(\frac{\partial q_0}{\partial z} - \frac{\partial q_e}{\partial z}\right)}{(q_0 - q_e)} dz\right)$$

to eliminate the first derivative. Again the general solution is obtained by separation of variables. In this case, the integral for time is taken over δt , an arbitrary time interval.

The boundary and initial condition for R from solution of equation [20] are still valid. Thus the final solution is identical in form to equation [23].

$$\hat{R} = \zeta \exp\left(\frac{\delta t}{\tau}\right)$$

It is desirable to use the τ_B defined in equation [23] in this solution because τ_B can be determined in the laboratory, and the influences of the physical properties of the porous media can be separated from the influence of the environment. Thus, if τ_B is used:

$$\hat{R} = \zeta \exp\left(\frac{\delta t}{\tau_B}\right) \quad [24]$$

In this case, ζ is not necessarily equal to 1 during the moisture exchange since it expresses the degree of nonhomogeneity when a new set of boundary conditions is applied.

The forms of equations [23] and [24] provide the basis for evaluating the numerical simulation. Neither equation provides the necessary detail to predict theoretically the operational coefficients required for vapor density or temperature flux.

The analytical solution for fixed boundary condition [equation 23] suggests that numerical solutions and laboratory experiments involving structurally homogeneous layers of litter and duff are required to define the timelags. The equations suggest that an exponential approach to equilibrium is to be expected. Since the initial vapor or temperature profiles are not homogeneous, a different response time should be expected for each different set of initial conditions. Thus, if the timelags as derived in the laboratory are to be extended to field applications, then a second coefficient expressing this nonhomogeneous initial state would be required. This step can be accomplished by either allowing the timelag to be environmentally dependent, or by allowing the new coefficient, ζ , to be variable. This paper is based on the more general solutions of a variable homogeneity coefficient with laboratory-derived timelags.

Relation of Timelag to Physical Properties

The analytical solutions presented above predicted an exponential approach to the equilibrium profile. If this process is valid in the more complex physical system found in nature, then the gain or loss of temperature and vapor density can be expressed through timelag determination. This timelag is directly related to the physical structure of litter and duff layers. The analytical solutions showed that the coefficients in the

exponent were related to the physical variables of layer thickness and bulk diffusivity.

If nondimensional groups of timelag, bulk or simple diffusivity, and thickness are formed, then a similarity number is defined as:

$$F_1 = \frac{\tau_B^D}{H^2} \quad [25]$$

which is readily recognized as the Fourier number (Gukhman 1965).

The complete model proposed in this paper includes a number of other variables. These are the diffusivity in the voids, and the particle timelag as well as the depth and horizon timelags. Also, since the particles exchange heat and vapor with the voids, the total mass of particles and their volume should also be considered. Three nondimensional groups of variables may be defined. The ratio of the bulk density to particle density—the packing ratio (β)—is one minus the porosity. The second group is the ratio of the system timelag to particle timelag. The third is composed of thickness of the system, the diffusivities in the voids, and a time variable. This time variable was chosen as the particle timelag since the descriptive model suggested this time interval as the critical time variable. The three groups are:

$$(\beta), \left(\frac{\tau_{PM}}{\tau_{BM}} \right), \left(\frac{v_B \tau_{PM}}{H^2} \right)$$

for mass exchange and

$$(\beta), \left(\frac{\tau_{PT}}{\tau_{BT}} \right), \left(\frac{k_B \tau_{PT}}{H^2} \right)$$

for heat exchange. These variables form similarity numbers of:

$$F_M = \left(\frac{\tau_{BM}}{\tau_{PM}} \right) \left(\frac{v_B \tau_{PM}}{H^2} \right)^{\frac{2}{3}} \beta^{-1} \quad [26]$$

and

$$F_T = \left(\frac{\tau_{BT}}{\tau_{PT}} \right) \left(\frac{k_B \tau_{PT}}{H^2} \right)^{\frac{2}{3}} \beta^{-1} \quad [27]$$

The packing ratio has been placed in the denominator of equations [26] and [27], since the timelag should increase as the bed porosity decreases. The Fourier number of the analytical solutions [equation 25]

may be similarly expressed for heat and vapor transfer. The Fourier number for heat transfer is:

$$\hat{F}_T = \frac{\tau_{BT} \hat{k}}{H^2} \quad [28]$$

and for water vapor

$$\hat{F}_M = \frac{\tau_{BM} \hat{v}}{H^2} \quad [29]$$

The hat ($\hat{}$) over the diffusivities in equations [28] and [29] denote the net value of the diffusivity obtained by neglecting the particle effect in diffusion experiments.

If the detailed theoretical results are a more general solution of the physical processes than those from simple diffusions, then the timelags predicted by either method should be the same for a given set of physical conditions.

Numerical Solution Methods

The analytical and similarity functions provided the basis for evaluating numerical solutions and observational data. The complete set of equations [1 through 6] must be solved simultaneously. Equations 1 and 4 are highly nonlinear and therefore must be solved numerically if the full dynamics are to be preserved.

Finite difference schemes must be adopted for both the spatial and temporal derivatives to solve these equations. The philosophy in describing the space derivatives was that certain regions of the system would require very high resolutions, while in others, the dynamic process would be slow and would not be characterized by strong gradients. Techniques utilizing a constant space interval would require the same high resolution in the quiescent regions as that desired in the strong-gradient, rapid-change regions. The finite difference scheme adopted allowed for arbitrarily selected space intervals between each computational point. This preserved the high resolution desired in certain regions, and reduced the total effort required to obtain a particular solution. The particular finite difference stencils adopted for the void to void diffusion are based on the mean value between each computational point. Thus, the first derivative of a scalar quantity (S) at a point i is:

$$\frac{\frac{S_{i+1} + S_i}{2} - \frac{S_i + S_{i-1}}{2}}{\frac{Z_{i-1} + Z_i}{2} - \frac{Z_i + Z_{i+1}}{2}}$$

where Z is the depth below the surface. If the computational points are equally spaced, then this scheme reduces to the familiar centered difference method. If the computational points are not equally spaced and the redundant value at i is eliminated, then the derivative is not defined at the point i . The second derivative is defined by the difference between the uncentered first derivatives

$$\frac{(S_{i+1} - S_i)}{(Z_i - Z_{i+1})} = D_u$$

and

$$\frac{(S_i - S_{i-1})}{(Z_{i-1} - Z_i)} = D_D$$

so that the second derivative is:

$$\frac{(D_u - D_D)}{\left(\frac{Z_{i-1} + Z_i}{2} - \frac{Z_{i+1} + Z_i}{2}\right)}$$

This derivative also reduces to the familiar centered second derivative with equally spaced computational points.

The finite difference time step used in this analysis was the Adams-Bashforth Scheme (Lilly 1965):

$$S_{i,t+1} = S_{i,t} + \left(\frac{3}{2} \left(\frac{\Delta S_i}{\Delta t} \right)_t - \frac{1}{2} \left(\frac{\Delta S_i}{\Delta t} \right)_{t-1} \right) \delta t$$

where the subscripts $t+1$, t , and $t-1$ refer to the new time, current time, and previous time, separated by the time interval δt . This scheme was chosen because of well defined stability in nonlinear thermofluid dynamic solutions.

The time step δt must be made sufficiently small so that the characters of the continuous equations are preserved with a minimum of distortion. The maximum value of δt is then defined by linear stability criteria of

$$\delta t_{\max} < \left(\frac{\delta z_i}{2D_i} \right)_{\min}$$

where δz is the distance between computational points and D is the diffusivity of heat or vapor in the void to void exchange.

A second constraint not related to computational stability, must be placed on the magnitude of the time step. This constraint arises because of the large

differences between the internal diffusivities of the particles and those in the voids. This constraint is not a mathematical or physical constraint, but is directly related to the resolution obtainable in digital computers and to the range over which the particle homogeneity coefficient is properly defined. If the two differential equations describing the heat and mass processes in the particles are included with those describing bed processes, then the number of computations that must be made becomes extremely large and beyond capabilities of even the largest computers. Computational limits are imposed by the modified analytical solution [equations 3 and 6]. This restriction is covered by ζ defined only over a small range of $\frac{\delta t}{\tau}$. The net effect is to increase stability. This tradeoff increases the number of time steps, but drastically decreases the total number of computations to the point that a net gain is obtained and practical solutions are possible.

Results of the Computations

The physical properties of litter and duff required to carry out the numerical simulations were the depth of the horizon, bulk density, particle density, thermal and moisture timelags of the particles, specific heat of the particles, and the equilibrium moisture isotherms.

The two species for which a complete analysis was carried out were ponderosa pine (*Pinus ponderosa*) and lodgepole pine (*Pinus contorta*). The particle densities for ponderosa pine were obtained from Brown (1970), and for lodgepole pine through personal correspondence with him.⁵ The moisture timelags and equilibrium moisture isotherms of both species for freshly fallen and weathered needles were obtained from Blackmarr through personal correspondence or unpublished research (see footnote 4). The thermal timelags were calculated from the relations developed previously (Fosberg 1973). The specific heat was given by equation [10]. The bulk densities of the horizons were obtained from samples collected on the Manitou and Fraser Experimental Forests of the Rocky Mountain Forest and Range Experiment Station, and on the Pingree Park Campus of Colorado State University. The ponderosa pine data came only from the Manitou Experimental Forest, while the lodgepole pine data came from all three areas. Data used in the simulations are summarized in table 1.

These data are supplemented through arbitrarily chosen variations for each physical property. Each of three physical variables—depths, bulk density, and particle timelag—were systematically varied over a large range of conditions while the others were held constant. The depths were selected as 1, 3, 4, 6, and 8 cm. The selected particle timelags were 3,600 seconds, 7,200 seconds, and the measured 4,608 seconds. While bulk densities of litter are mostly

⁵Brown, J. K. October 11, 1972, personal correspondence.

Table 1.--Physical properties of duff and litter horizons

Horizon	Particle timelags (sec.)		Density (gm cm ⁻³)	
	Moisture (τ_M)	Thermal (τ_T)	Particle (ρ_p)	Bed bulk (ρ_B)
<u>Ponderosa Pine</u>				
Litter A _{oo}				
Freshly fallen needles	14,760	0.12	0.51	0.08
Weathered needles	4,608	.11	.47	.08
Duff A _o	--	--	.47	.26
<u>Lodgepole Pine</u>				
Litter A _{oo}				
Freshly fallen needles	63,000	.10	.56	.09
Weathered needles	3,636	.10	.56	.09
Duff _o	--	--	.56	.36

in the range of 0.06 to 0.1 gm/cm³, the mean value of 0.08 gm/cm³ was supplemented with bulk densities 0.01, 0.02, and 0.03 gm/cm³ to provide a larger range of values to evaluate the similarity numbers.

The individual computer simulations using equations [1] through [12] for a particular value of particle and bed properties were evaluated through the characteristics provided by the analytical solutions [equations 23 and 24], and by the similarity relations predicted by equations [26] and [29].

The first set of simulation results applies to a constant environment. These simulated results defined the timelag characteristics and provided the functions to predict them from observations of the physical structure.

The second set of simulation results utilizes the predicted constant responses and applies them to prediction of heat and moisture response with time-dependent boundary conditions. This second set of results provides the framework for field prediction.

Constant Boundary Conditions

The numerical simulations of these conditions were conducted under the conditions of an initially

homogeneous moisture and temperature. At an arbitrary time zero, an arbitrary step change of either relative humidity or temperature was imposed while the other boundary was held at its original value. The step change in the boundary condition then set up a time-dependent process from the initial homogeneous state to one in which the final equilibrium profile was a linear function with depth. The time-dependent approach to the equilibrium could then be used to determine the timelag of the complete system. As examples, several of the simulations for moisture exchange are shown here to illustrate the details of the nonlinear solutions.

The first set of examples is for isothermal conditions. Boundary conditions were set at 20 percent relative humidity at the surface, and the initial homogeneous void relative humidity was 80 percent. The temperature was 300 K. Particle and bed properties were defined by weathered ponderosa pine litter. The depths of the two horizons were arbitrarily selected as 3 and 4 cm (reasonable values for stands of basal area in the 15 to 20 m²/hectare range along Colorado's east slope).

Initial moisture properties were used to evaluate the timelags. The integral particle moisture content for the two examples (fig. 2) follows the expected exponential decay. The 3-cm-thick layer had a timelag of

Particle moisture
content (percent)

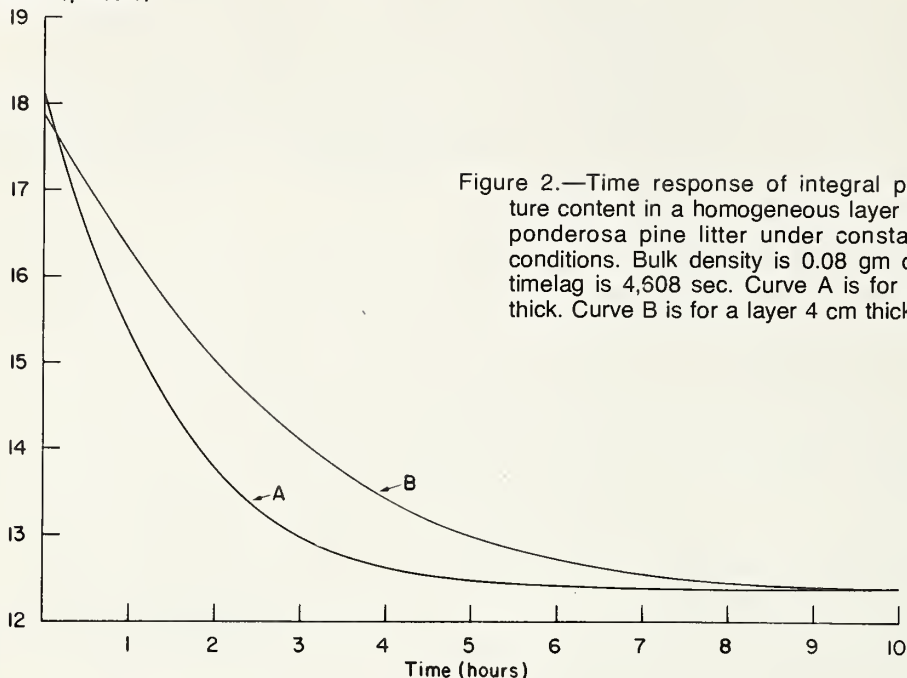


Figure 2.—Time response of integral particle moisture content in a homogeneous layer of weathered ponderosa pine litter under constant boundary conditions. Bulk density is 0.08 gm cm^{-3} . Particle timelag is 4,608 sec. Curve A is for a layer 3 cm thick. Curve B is for a layer 4 cm thick.

4,248 seconds while the 4-cm layer had a timelag of 7,560 seconds. The integral of void vapor density (fig. 3) for the two cases also showed the exponential

decay, and had timelags nearly identical to those for particle moisture content. Void vapor density was chosen to represent the moisture transport since the

$\rho (10^{-6} \text{ gm/cm}^3)$

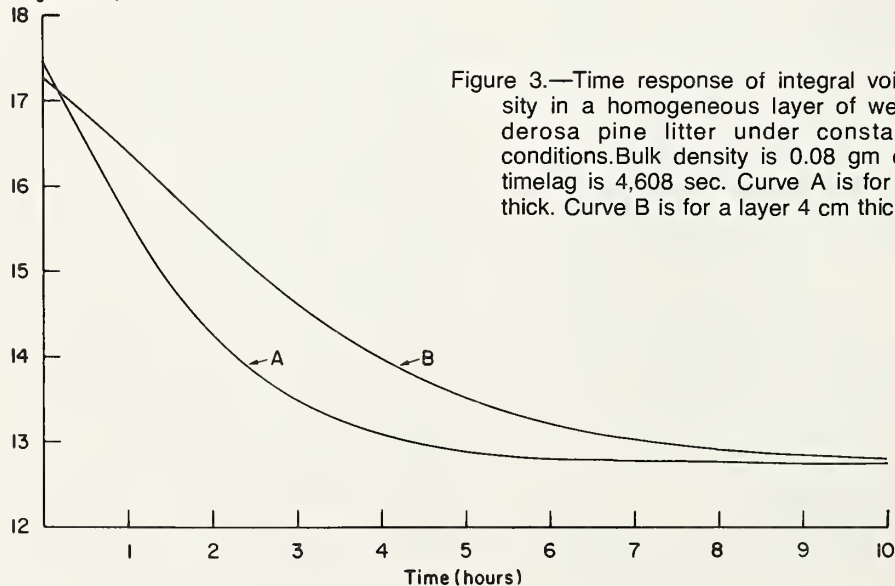


Figure 3.—Time response of integral void vapor density in a homogeneous layer of weathered ponderosa pine litter under constant boundary conditions. Bulk density is 0.08 gm cm^{-3} . Particle timelag is 4,608 sec. Curve A is for a layer 3 cm thick. Curve B is for a layer 4 cm thick.

equilibrium moisture content of the particles is a non-linear function of relative humidity, and because relative humidity is strongly dependent on temperature. Void relative humidity profiles for the two examples (fig. 4) decayed rapidly to the linear equilibrium profile. The particle moisture content profiles (fig. 5) can be predicted from the void vapor density and

the temperature, since the vapor density and the moisture content approach equilibrium at the same rate.

Temperature in the duff and litter layer changed much more rapidly than moisture. The integral temperature change over time also approached equilibrium exponentially (fig. 6). Surface boundary conditions for the temperature experiments were 290, 296, 305, and

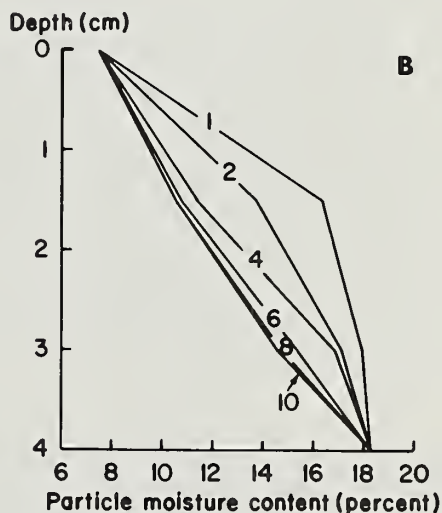
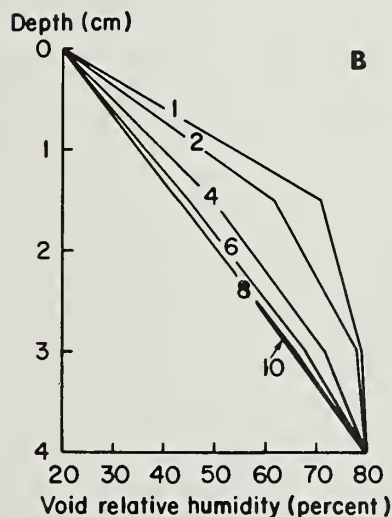
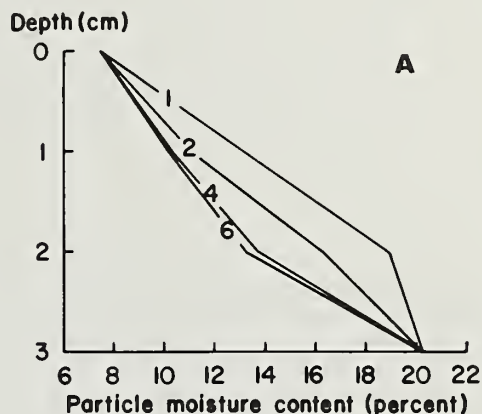
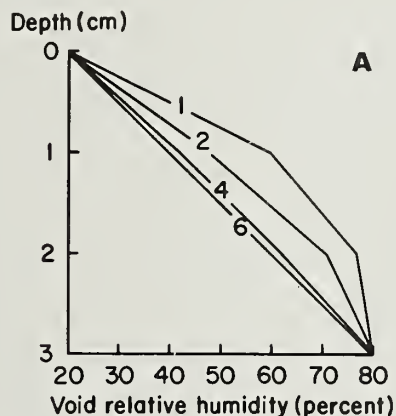
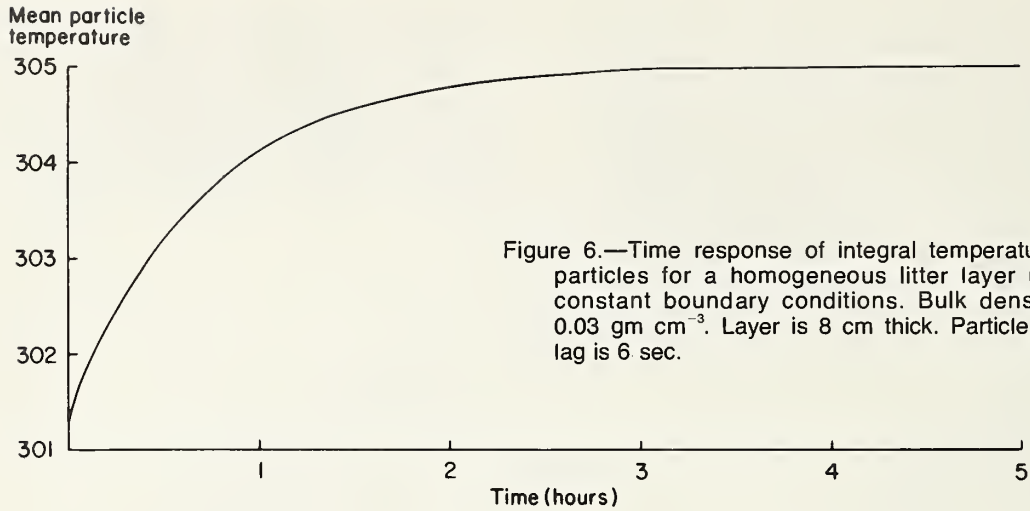


Figure 4.—Profiles of void relative humidity for weathered ponderosa pine litter under constant boundary conditions. Bulk density is 0.08 gm cm^{-3} . Particle timelag is 4,608 sec. Numbers on lines indicate hours since beginning of solution. A is for a layer 3 cm thick; B is for a layer 4 cm thick.

Figure 5.—Profiles of particle moisture content for weathered ponderosa pine litter under constant boundary conditions. Bulk density is 0.08 gm cm^{-3} . Particle timelag is 4,608 sec. Numbers on lines indicate hours since beginning of solution. A is for a layer 3 cm thick; B is for a layer 4 cm thick.



310 K. The initial temperatures were 300 K. Initial and boundary condition relative humidities were 20 percent. Profiles of temperature (fig. 7) behaved similarly to those for vapor density in that their equilibrium profiles were linear. When both moisture and temperature boundary condition changes were imposed, the vapor density profiles still decayed to the linear equilibrium profile (fig. 8). The relative humidity boundary condition was 20 percent and the temperature boundary condition was 310 K. Initial conditions were 80 percent relative humidity and 300 K. The internal maximum of vapor density represents the thermally driven moisture flux. Thus, the conservative nature of temperature and vapor density provides a more stable basis for predicting moisture content than methods based on relative humidity.

The individual results of the 25 simulations where each bed and particle property was systematically varied were combined by the similarity results defined by equations [26] and [27]. These similarity relations provided the basis for predicting the horizon timelags from the physical properties of particles and bed. The vapor density relationship was:

$$F_M = 196 = \frac{\tau_{BM} v_{BM}^{\frac{2}{3}}}{H^{\frac{4}{3}} \tau_{PM}^{\frac{1}{3}} (1-\phi)} \quad [30]$$

and is graphically shown in figure 9. Similarly the relationship for heat transfer is

$$F_T = 309 = \frac{\tau_{BT} k_{BT}^{\frac{2}{3}}}{H^{\frac{4}{3}} \tau_{PT}^{\frac{1}{3}} (1-\phi)} \quad [31]$$

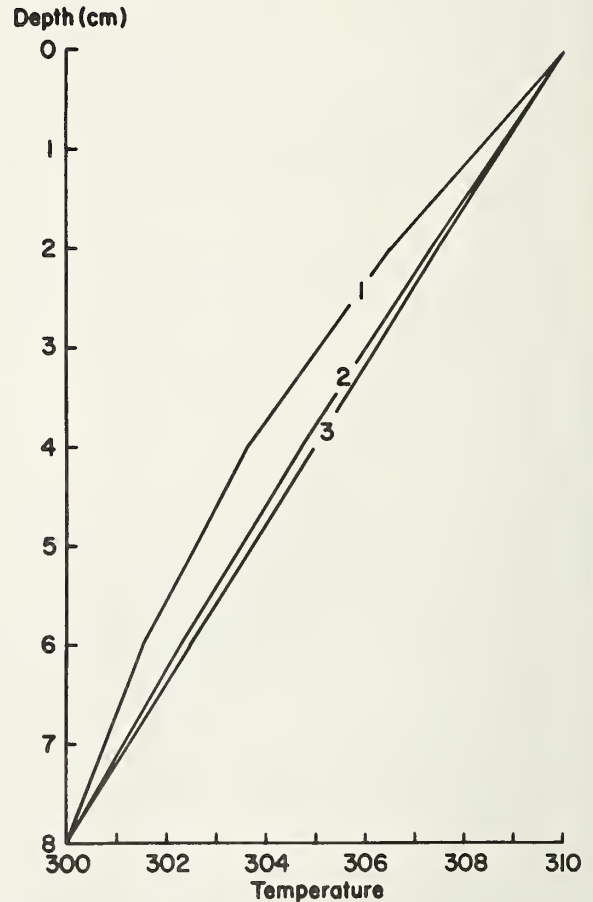
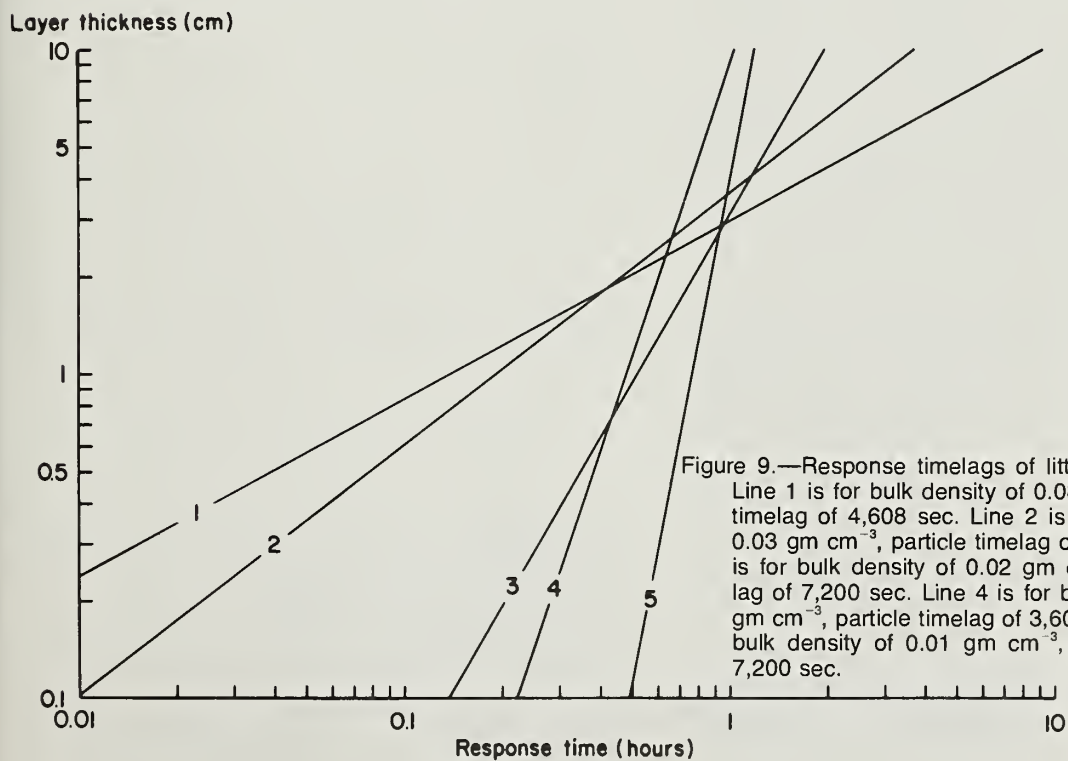
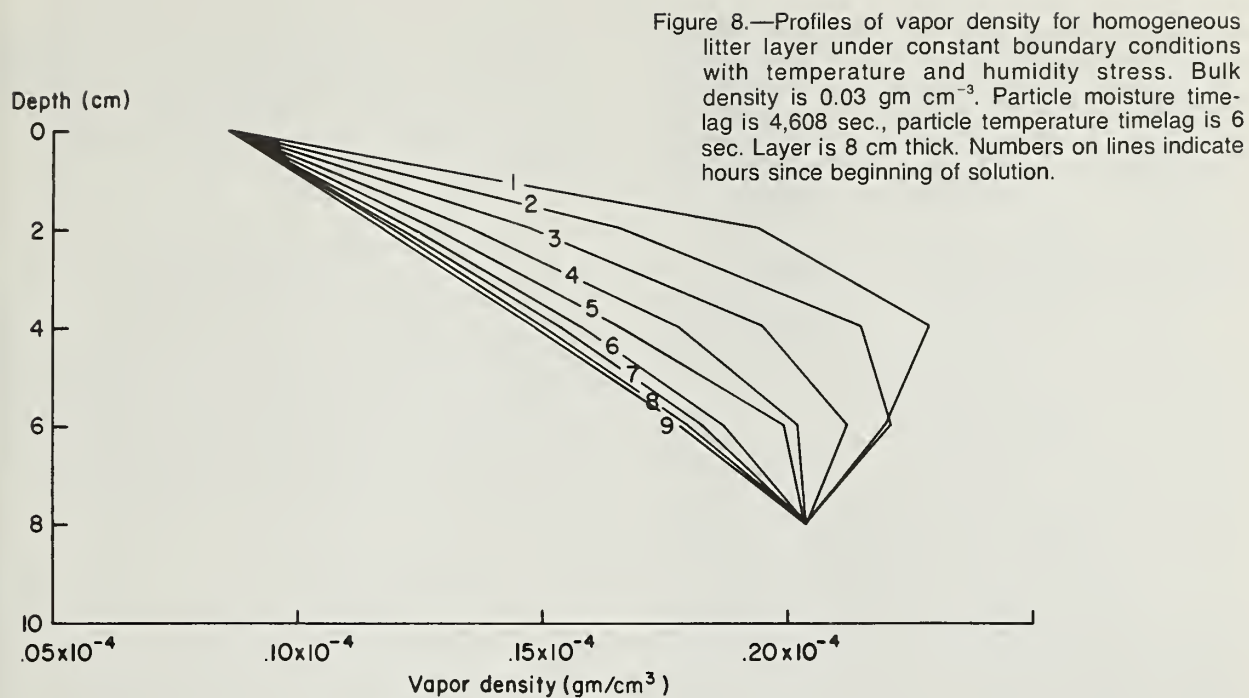


Figure 7.—Profiles of particle temperature for homogeneous litter layer under constant boundary conditions. Bulk density is 0.03 gm cm^{-3} . Layer is 8 cm thick; particle time-lag is 6 sec. Numbers on lines indicate hours since beginning of solution.



The similarity numbers of equations [30] and [31] are averages of the individual simulations. The range of the similarity numbers was 20 percent of the mean for mass transfer and 10 percent for heat transfer. These two similarity relations provided the basis for calculating the moisture and temperature time-lags under constant or laboratory conditions.

Time-Dependent Boundary Conditions

The natural environment rarely provides constant boundary conditions. More typically, the boundary conditions are continuously changing temperatures and humidities. Functions must therefore be established for these variations under which the horizons do not reach an equilibrium state. As with the constant environment case, the analytical solutions provide the functional framework for evaluation of numerical solutions. Laboratory and field solutions differ only by a linear multiplier of the exponential terms. This linear coefficient reflects the inhomogeneity of the initial conditions. The coefficient ζ of equation [24] would be unity under constant boundary conditions, but will be different from unity under nearly all field conditions.

The time-dependent boundary conditions were defined by step changes of arbitrary duration and arbitrary magnitude. These changes established a nonhomogeneous interval profile. The integral vapor density (fig. 10) and the integral temperature (fig. 11) change over time show two marked characteristics. The responses of the layers are much more rapid when they start from the nonhomogeneous profile than when they start from the homogeneous profile. This difference can be interpreted either as a change in the timelag or as enhanced transport due to larger gradients. Because the timelag was defined in terms of physical properties, the second interpretation is preferred. This latter interpretation has the advantage that dynamic and physical characteristics are separated in the functions.

The coefficient ζ of equation [24] then must be defined for the heat and mass transfers. This was accomplished by calculating the actual change in vapor density or temperature, the potential change in vapor density or temperature, and using the timelags defined from the constant boundary condition simulation. This ζ is:

$$\zeta = \frac{1 - \frac{\delta S}{\Delta S}}{\exp - \frac{t_d}{\tau}}$$

where δS is the actual change of the scalar quantity, ΔS is the potential change, and t_d is the duration of the pulse.

The homogeneity coefficient for mass transfer is 0.42 and for heat transfer is 0.755. No variation of the coefficient was found in the simulation used to determine these values. Variation probably does exist and would be found if more simulation or field experiments are conducted.

Comparison of Generalized Solutions with Fickian Solutions

Bulk diffusivities of the horizons can be used to validate the theoretical predictions. These bulk diffusivities can be calculated from the two pairs of similarity equations. By solving equations [29] and [30] for τ_{BM} and equations [27] and [31] for τ_{BT} , the bulk vapor diffusivity \hat{v} and thermal diffusivity \hat{k} can be calculated. The effective vapor diffusivity is:

$$\hat{v} = \frac{0.18 (H v_B)^{\frac{2}{3}}}{196 \tau_{PM}^{\frac{1}{3}} \beta}$$

and the effective thermal diffusivity is:

$$\hat{k} = \frac{0.14 (H k_B)^{\frac{2}{3}}}{309 \tau_{PT}^{\frac{1}{3}} \beta}$$

The coefficients 0.18 and 0.14 are taken from Fosberg (1972, 1973).

The vapor diffusivity for the example in figures 2 through 5 is:

$$3.1 \times 10^{-4} \text{ cm}^2/\text{sec.}$$

The thermal diffusivity for the temperature change of figure 6 is:

$$5.7 \times 10^{-3} \text{ cm}^2/\text{sec.}$$

These bulk diffusivities compare well with experimental values based on equilibrium solutions (Lettau 1954; Jackson 1964a, 1964b, 1964c).

Reported moisture response rates for litter and duff have typically been very slow. Johnson's (1968) analysis of field data gives timelags an order of magnitude greater than reported here. Since Van Wagner (1970) used the timelag as the environment dependent variable, it is difficult to determine the exact magni-

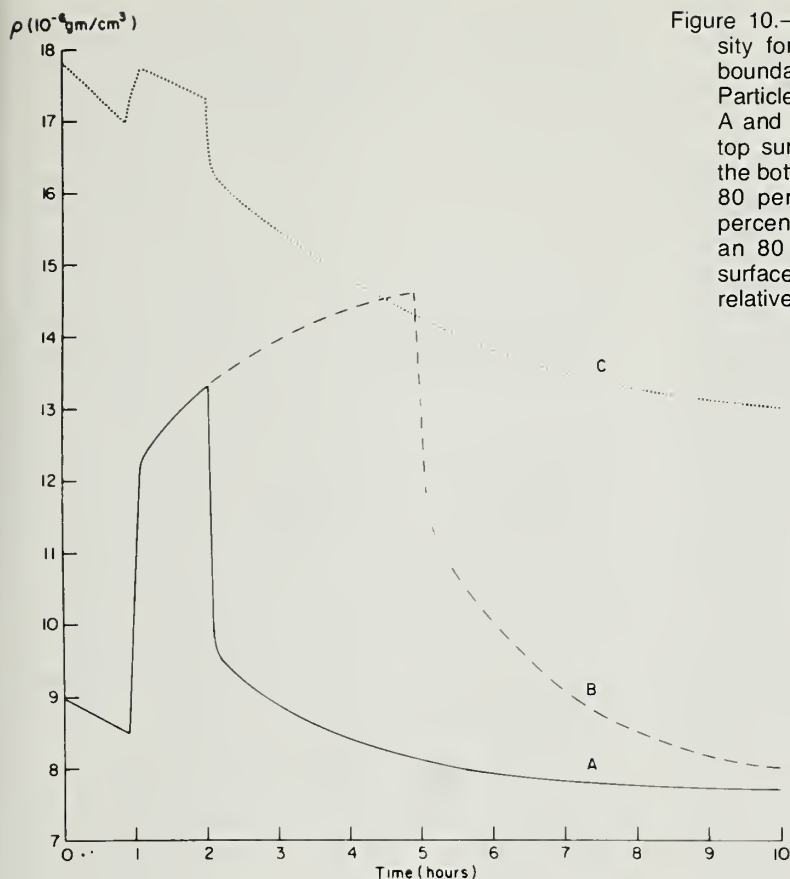


Figure 10.—Time response of integral void vapor density for homogeneous litter layers under varying boundary conditions. Bulk density is 0.03 gm cm^{-3} . Particle timelag is 3,600 sec. Thickness is 8 cm. Lines A and B had a 20 percent relative humidity on the top surface and a 40 percent relative humidity on the bottom surface. The top surface was changed to 80 percent relative humidity. Line C had a 20 percent relative humidity on the top surface and an 80 percent relative humidity on the bottom surface. The top surface was changed to 40 percent relative humidity.

tude of the structure timelag. Examination of the forcing and response functions suggests a magnitude similar to that reported by Johnson (1968).

Data used by Johnson (1968) and Van Wagner (1970) come from observations taken once a day. Thus, the reported responses were artificially forced to long timelags since the minimum resolvable timelag cannot be less than 1 day. Data collected at high sample rates⁶ show high response rates and short timelags similar to those predicted by the theoretical solutions. Thus, discrepancies between the theoretical solution and timelag values previously reported are due to artificial filtering created through sampling procedures.

Comparisons of the theoretical prediction to observation were made with Nelson's (1969) experimental results in sawdust layers. The theory predicted a timelag of 360 minutes, while Nelson observed timelags that ranged from 390 to 420 minutes for low moisture timelags. Measured timelags of ponderosa

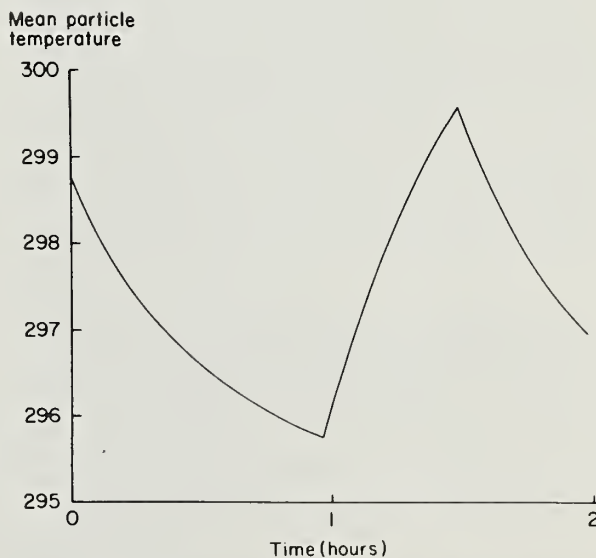


Figure 11.—Time response of integral particle temperature for homogeneous litter layer under varying boundary conditions. Bulk density is 0.03 gm cm^{-3} . Particle timelag is 6 sec. Layer is 8 cm thick.

⁶McLeod, Bruce. December 7, 1973, *Microwaves, a new tool for forest and watershed management*. 15 p. (Unpublished report, Mont. State Univ., Bozeman.)

pine needles in loosely packed beds⁷ were close to those predicted by the theoretical solutions.

Conclusions

The theoretical model developed in this paper is a generalization of previously derived theoretical solutions. The improvement over traditional solutions was obtained by following the physical processes more closely. Three main quantitative results were obtained from the theoretical predictions.

The first was the prediction of timelags from physical properties of particles and from horizon structure. These thermal and vapor timelags provide basic coefficients for analytical predictions of heat and vapor exchanges. Thermal and vapor timelags cannot be calculated as the particle timelags go to zero. Nonsorbing porous media flow is depicted by the simple analytical solution and similarity is not preserved. While this limitation indicates that the solutions are not completely generalized, calculations over the range of properties in organic soils are valid.

The second primary result was two pairs of prediction equations. The first pair apply to heat and vapor changes with constant boundary conditions and initially homogeneous profiles. These equations depict the behavior of the horizons in the laboratory. The second pair of equations for heat and vapor change prediction relax the requirement of initially homogeneous profiles and constant boundary conditions. This pair of equations depicts the processes under natural or field conditions of temperature and moisture profiles.

These solutions for field conditions permit a variable set of boundary conditions. The equation requires surface temperature and the vapor density at the surface. Because the boundary conditions are held constant over a small integration interval, but can vary between finite intervals, the boundary conditions are actually finite difference approximations to the continuous change. The homogeneity coefficient in these field-applicable equations reflects the departure of the initial state from homogeneous temperature and moisture profiles. If most of the changes in temperature

and moisture are determined by surface boundary conditions, then the homogeneity coefficient will be less than one. A coefficient of less than one then indicates a deep, slowly changing reservoir. A coefficient of one applies only in the laboratory. Coefficients greater than one indicate quiescent surface conditions, with most of the change taking place in the deeper horizons.

The third quantitative result was the recalculation of the bulk diffusivities for nonsorbing particles. These bulk diffusivities are the same as those traditionally determined in the laboratory, and are based on the assumption of instantaneous response of the particles.

The model requires horizon thickness, porosities, and particle timelags to make the predictions. The particle timelags must be determined in the laboratory. Neither particle timelags nor densities vary much between samples. Bulk densities of each horizon also vary within a narrow range, so the porosity can be calculated from the particle and bulk densities. Horizon depth varies widely even in small plots of constant basal area, so that there is a large potential uncertainty in extrapolation of an individual calculation to different sites. The only other data requirements of the model are the boundary conditions. These data are the temperature and atmospheric moisture content at the upper surface.

The model can be applied to forestry problems such as fire danger by specifying the physical properties of thickness, particle timelag, and porosity. With these data the vapor and thermal timelags can be calculated. The field prediction equations are then solved sequentially for each horizon. The external boundary conditions of surface temperature and vapor density apply to the surface horizon. The temperature and vapor density boundary conditions for internal horizons are specified by the vapor density and temperature of the adjacent higher horizon. The lowest horizon must be selected sufficiently deep—such as below the depth of diurnal fluctuation for prediction extending a few days or below the depth of annual fluctuation for seasonal calculation—to eliminate the lower boundary condition. Since the moisture content timelag and vapor density timelag are nearly identical, the moisture content profiles can be calculated directly from the equilibrium moisture isotherms. These theoretical solutions do not contain liquid water processes. Addition of liquid water can be considered through minor modification of classic infiltration theory and therefore complete the model of practical application.

⁷Anderson, Hal. E., Robert W. Mutch, and Robert D. Schuette. 1975. *Timelag and equilibrium moisture content of ponderosa pine needles*. 20 p. (Unpublished manuscript, U.S. For. Serv., Missoula, Mont.)

Literature Cited

- Ayres, K. W., R. G. Button, and E. De Jong.
1972. Soil morphology and soil physical properties. I. Soil aeration. *Can. J. Soil Sci.* 52:311-321.
- Baver, L. D.
1956. *Soil physics*. John Wiley. New York. 489 p.
- Blackmarr, W. H.
1971. Equilibrium moisture content of common fine fuels found in southeastern forest. USDA For. Serv. Res. Pap. SE-74, 8 p., Southeast For. Exp. Stn., Asheville, N.C.
- Brown, James K.
1970. Physical fuel properties of ponderosa pine forest floors and cheatgrass. USDA For. Serv. Res. Pap. INT-74, 16 p., Intermt. For. and Range Exp. Stn., Ogden, Utah.
- Childs, E. C.
1969. An introduction to the physical basis of soil water phenomena. John Wiley and Sons. New York. 493 p.
- Chudnovskii, A. F.
1962. Heat transfer in the soil. *Israel Prog. Sci. Trans.* Jerusalem. 164 p.
- Clary, Warren P., and Peter F. Ffolliott.
1969. Water holding capacity of ponderosa pine forest floor layers. *J. Soil Water Conserv.* 24:22-23.
- Currie, J. A.
1960a. Gaseous diffusion in porous media. Part I—A non-steady state method. *Brit. J. Appl. Phys.* 11:314-317.
- Currie, J. A.
1960b. Gaseous diffusion in porous media. Part II—Dry granular materials. *Brit. J. Appl. Phys.* 11:318-324.
- Currie, J. A.
1961. Gaseous diffusion in porous media. Part III—Wet granular materials. *Brit. J. Appl. Phys.* 12:275-281.
- De Jong, E., and H. J. V. Schappert.
1972. Calculation of soil respiration and activity from CO₂ profiles in the soil. *Soil Sci.* 113:328-333.
- Fosberg, Michael A.
1970. Drying rates of heartwood below fiber saturation. *For. Sci.* 16:57-63.
- Fosberg, Michael A.
1972. Theory of precipitation effects on dead cylindrical fuels. *For. Sci.* 18:98-108.
- Fosberg, Michael A.
1973. Prediction of prepyrolysis temperature rise in dead forest fuels. *Fire Technol.* 9:182-188.
- Gast, P. R., and P. W. Stickel.
1929. Solar radiation and relative humidity in relation to duff moisture and forest fire hazard. *Mon. Weather Rev.* 57:466-468.
- Gukhman, A. A.
1965. *Introduction to the theory of similarity*. Academic Press. New York. 256 p.
- Hanks, R. J.
1958. Water vapor transfer in dry soil. *Soil Sci. Soc. Am. Proc.* 22:372-374.
- Harkness, H. W.
1939. On the time required for forest duff to attain hygroscopic equilibrium. *For. Chron.* 15:164-171.
- Jackson, Ray D.
1964a. Water vapor diffusion in relatively dry soil: I. Theoretical considerations and sorption experiments. *Soil Sci. Soc. Am. Proc.* 28:172-176.
- Jackson, Ray D.
1964b. Water vapor diffusion in relatively dry soil: II. Desorption experiments. *Soil Sci. Soc. Am. Proc.* 28:464-466.
- Jackson, Ray D.
1964c. Water vapor diffusion in relatively dry soil: III. Steady-state experiments. *Soil Sci. Soc. Am. Proc.* 28:467-470.
- Jarvis, J., and R. E. Tucker.
1968. Drought index as a predictor of moisture content in L and F horizons on an upland white spruce-trembling aspen cut-over area. *For. Branch Dep. Publ.* 1237, 10 p.
- Johnson, Von J.
1968. Buildup index as an expression of moisture content in duff. USDA For. Serv. Res. Note NC-43, 4 p., North Cent. For. Exp. Stn., St. Paul, Minn.
- Lettau, Heinz.
1954. Improved models of thermal diffusion in the soil. *Trans. Am. Geophys. Union* 35:121-132.
- Lilly, Douglas K.
1965. On the computational stability of numerical solutions of time-dependent nonlinear geophysical fluid dynamics problems. *Mon. Weather Rev.* 93:11-26.
- List, Robert J.
1966. *Smithsonian meteorological tables*. Smithsonian Inst. Publ. 4014. Wash. D.C. 527 p.
- Millington, R. J.
1959. Gas diffusion in porous media. *Science* 130:100-102.
- Millington, R. J., and R. C. Schearer.
1971. Diffusion in aggregated porous media. *Soil Sci.* 111:372-378.

- Miyamoto, S., J. Letey, and J. Osborn.
1972. Water vapor adsorption by water-repellent soils at equilibrium. *Soil Sci.* 114:180-184.
- Muraro, S. J., and B. D. Lawson.
1970. Prediction of duff moisture for prescribed burning. *For. Res. Lab., Can. For. Serv., Inf. Rep. BC-X-46*, 13 p. Victoria, B.C.
- Mutch, R. W., and O. W. Gastineau.
1970. Timelag and equilibrium moisture content of reindeer lichen. *USDA For. Serv. Res. Pap. INT-76*, 8 p., Intermt. For. and Range Exp. Stn., Ogden, Utah.
- Nelson, Ralph M., Jr.
1969. Some factors affecting the moisture timelags of woody materials. *USDA For. Serv. Res. Pap. SE-44*, 16 p., Southeast For. Exp. Stn., Asheville, N. C.
- Penman, H. L.
1940. Gas and vapor movement in the soil. I. The diffusion of vapors through porous solids. *J. Agric. Sci.* 30:437-462.
- Siau, John F.
1971. *Flow in wood*. Syracuse Univ. Press. Syracuse, N.Y. 131 p.
- Taylor, Sterling A.
1949. Oxygen diffusion in porous media as a measure of soil aeration. *Soil Sci. Soc. Am. Proc.* 14:55-61.
- U. S. Department of Agriculture, Forest Products Laboratory.
1974. *Wood Handbook*. U. S. Dep. Agric., Agric. Handb. 72, rev., n.p.
- Van Wagner, C. E.
1969. Drying rates of some fine forest fuels. *Fire Control Notes* 30(4):5, 7, 12.
- Van Wagner, C. E.
1970. An index to estimate the current moisture content of the forest floor. *Dep. Fish and For., Can. For. Serv. Publ.* 1288, 23 p.

Appendix—List of Symbols

Symbol	Definition	Units
C_p	Specific heat of air constant pressure	$\text{cal gm}^{-1} \text{ }^\circ\text{K}^{-1}$
e	Vapor pressure in air	dynes cm^{-2}
e_s	Saturation vapor pressure	dynes cm^{-2}
F_M	Similarity number for moisture transfer in litter and duff	dimensionless
\hat{F}_M	Similarity number for moisture transfer in nonsorbing porous media	dimensionless
F_T	Similarity number for heat transfer in litter and duff	dimensionless
\hat{F}_T	Similarity number for heat transfer in nonsorbing porous media	dimensionless
H	Thickness of a homogeneous horizon	cm
h	Relative humidity	percent
k_B, k	Thermal diffusivity in voids	$\text{cm}^2 \text{ sec}^{-1}$
k_o	Thermal diffusivity in free air	$\text{cm}^2 \text{ sec}$
\bar{k}	Effective thermal diffusivity in litter or duff	$\text{cm}^2 \text{ sec}^{-1}$
M_a	Mass of air in litter or duff volume	gm
M_F	Mass of litter particles in litter or duff volume	gm
m	Moisture content of litter or duff (mass of contained water to oven-dry mass of particle)	percent
m_e	Equilibrium moisture content	percent
m_i	Initial moisture content	percent
q	Arbitrary scalar variable	dimensionless
q_e	Equilibrium value of arbitrary scalar	dimensionless
q_o	Initial value of arbitrary scalar	dimensionless
R	Gas constant for water vapor	$\text{cal gm}^{-1} \text{ }^\circ\text{K}^{-1}$
s	Source or sink of heat in litter or duff	cal
T	Temperature in litter or duff	deg K
t	Time coordinate	sec

Appendix—List of Symbols (Continued)

Symbol	Definition	Units
V_B	Volume of litter or duff	cm^3
V_F	Volume of particles in litter or duff	cm^3
V_v	Volume of voids in litter or duff	cm^3
z	Vertical space coordinate	cm
β	Packing ratio (1 - porosity)	dimensionless
Δm	Potential change of particle moisture content	percent
ΔT	Potential change of particle temperature	deg K
δH_a	Change of heat in litter or duff voids	cal
δH_F	Change of heat in litter or duff particles	cal
δm	Change of moisture content in particles	percent
$\delta T_F, \delta T$	Change of temperature in particles	deg K
δt	Finite time step	sec
ζ_M	Homogeneity coefficient for moisture transfer	dimensionless
ζ_T	Homogeneity coefficient for heat transfer	dimensionless
ρ_a	Density of air	gm cm^{-3}
ρ_B	Bulk density of litter or duff	gm cm^{-3}
ρ_f	Density of litter or duff particles	gm cm^{-3}
ρ_v	Water vapor density in voids	gm cm^{-3}
$\rho_{\check{v}}$	Water vapor density equivalent of moisture in particles	gm cm^{-3}
τ_{BM}	Moisture timelag of homogeneous horizon of litter or duff	sec
τ_{BT}	Thermal timelag of homogeneous horizon of litter or duff	sec
τ_{PM}	Moisture timelag of litter or duff particle	sec
τ_{PT}	Thermal timelag of litter or duff particle	sec
ν, ν_B	Moisture diffusivity in voids	$\text{cm}^2 \text{sec}^{-1}$
ν_o	Moisture diffusivity in free air	$\text{cm}^2 \text{sec}^{-1}$

Appendix—List of Symbols (Continued)

Symbol	Definition	Units
\dot{v}	Effective moisture diffusivity in litter or duff	$\text{cm}^2 \text{ sec}^{-1}$
ϕ	Porosity of litter or duff (Volume of voids/volume of horizon)	dimensionless
χ	Source or sink of moisture in litter or duff	percent



Fosberg, Michael A.

1975. Heat and water vapor flux in conifer forest litter and duff: a theoretical model. USDA For. Serv. Res. Pap. RM-152, 23p. Fort Collins, Colo. 80521.

The model was developed from numerical and analytical solutions of the diffusion forms of the mass continuity equation and the first law of thermodynamics. Analytical solutions provided a functional framework to evaluate nonlinear interactions obtained in the numerical solutions. Dimensional analysis was used to define the relationships between the soil properties used in the model.

Keywords: Soil physics, forest fires, forest fuels.

Fosberg, Michael A.

1975. Heat and water vapor flux in conifer forest litter and duff: a theoretical model. USDA For. Serv. Res. Pap. RM-152, 23p. Fort Collins, Colo. 80521.

The model was developed from numerical and analytical solutions of the diffusion forms of the mass continuity equation and the first law of thermodynamics. Analytical solutions provided a functional framework to evaluate nonlinear interactions obtained in the numerical solutions. Dimensional analysis was used to define the relationships between the soil properties used in the model.

Keywords: Soil physics, forest fires, forest fuels.

Fosberg, Michael A.

1975. Heat and water vapor flux in conifer forest litter and duff: a theoretical model. USDA For. Serv. Res. Pap. RM-152, 23p. Fort Collins, Colo. 80521.

The model was developed from numerical and analytical solutions of the diffusion forms of the mass continuity equation and the first law of thermodynamics. Analytical solutions provided a functional framework to evaluate nonlinear interactions obtained in the numerical solutions. Dimensional analysis was used to define the relationships between the soil properties used in the model.

Keywords: Soil physics, forest fires, forest fuels.

Fosberg, Michael A.

1975. Heat and water vapor flux in conifer forest litter and duff: a theoretical model. USDA For. Serv. Res. Pap. RM-152, 23p. Fort Collins, Colo. 80521.

The model was developed from numerical and analytical solutions of the diffusion forms of the mass continuity equation and the first law of thermodynamics. Analytical solutions provided a functional framework to evaluate nonlinear interactions obtained in the numerical solutions. Dimensional analysis was used to define the relationships between the soil properties used in the model.

Keywords: Soil physics, forest fires, forest fuels.

